Fluid Dynamics & Materials Processing

Tech Science Press

DOI: 10.32604/fdmp.2022.019485

ARTICLE

Thermal Conductivity and Dynamic Viscosity of Highly Mineralized Water

Dadang Mohamad[1,*], Mohammed Abed Jawad[2], John William Grimaldo Guerrero[3], Tonton Taufik Rachman[4], Huynh Tan Hoi[5], Albert Kh. Shaikhlislamov[6], Mustafa M. Kadhim[7], Saif Yaseen Hasan[8] and A. Surendar[9]

[1]Building Engineering Educatation, Universitas Pendidikan Indonesia, Bandung, 45363, Indonesia

[2]Al-Nisour University College, Iraq, 10004, Baghdad

[3]Departamento de Energía, Universidad de la Costa, Barranquilla, 080002, Colombia

[4]Universitas Masoem, Bandung, 45363, Indonesia

[5]Department of Language, FPT University, Hanoi, 700000, Vietnam

[6]Kazan Federal University, Russia, Kazan, 420000, Russia

[7]Dentistry Department, Kut University College, Kut, Wasit, Iraq, College of Technical Engineering, The Islamic University, Najaf, 54001, Iraq

[8]National University of Science and Technology, Dhi-Qar, 64001, Iraq

[9]Department of Pharmacology, Saveetha Dental College and Hospital, Saveetha Institute of Medical and Technical Sciences, Chennai, 600056, India

[*]Corresponding Author: Dadang Mohamad. Email: m.mana.qeshm@gmail.com

Received: 26 September 2021 Accepted: 09 November 2021

ABSTRACT

Further development in the field of geothermal energy require reliable reference data on the thermophysical properties of geothermal waters, namely, on the thermal conductivity and viscosity of aqueous salt solutions at temperatures of 293–473 K, pressures Ps = 100 MPa, and concentrations of 0–25 wt.%. Given the lack of data and models, especially for the dynamic viscosity of aqueous salt solutions at a pressure of above 40 MPa, generalized formulas are presented here, by which these gaps can be filled. The article presents a generalized formula for obtaining reliable data on the thermal conductivity of water aqueous solutions of salts for Ps = 100 MPa, temperatures of 293–473 K and concentrations of 0%–25% (wt.%), as well as generalized formulas for the dynamic viscosity of water up to pressures of 500 MPa and aqueous solutions of salts for Ps = 100 MPa, temperatures 333–473 K, and concentration 0%–25%. The obtained values agree with the experimental data within 1.6%.

KEYWORDS

Thermal conductivity; dynamic viscosity; water-salt systems; aqueous solutions of salts; high pressure; multicomponent water-salt systems

1 Introduction

For many years, solutions have attracted and continue to attract the attention of many researchers due to the important role they play in all natural phenomena of life and the complexity of their nature that is largely determined by the properties of the liquid phase in general. The development of power engineering and other

industries is closely related to the use of a wide range of coolants and working fluids. Among the liquid heat carriers used in various sectors of the economy, aqueous and non-aqueous solutions of inorganic substances play an important role [1–6]. The use of suitable nano additives to improve and increase the cooling property in industrial devices can be effective in reducing the hot spot temperature, which is one of the design limitations [7,8]. It increases the nominal power, reduce the dimensions and consumables in equipment as coolant. Studies on nanofillers show that increasing the thermal conductivity of nanofluids depends on many variables [9–12]. These factors include nano-filler size, particle surface shape and area, filler volume, particle aggregation, stability, viscosity, brown motion and temperature effect. In this paper, these factors are introduced and how they affect the heat transfer of nanofluids. In one study, h-BN powder nanoparticles were used as fillers in ethylene glycol fluid [13]. After preparing nanofluids with filler values of 0.025 vol and 0.2% vol and examining their thermal conductivity, the results showed that the thermal conductivity for nanofluids with filler volume of 0.025% is higher than the other.

Aqueous solutions of electrolytes are widely used in power generation systems at thermal and nuclear power plants, plants using solar and geothermal energy, oil and gas industry. In such industries as the production of mineral fertilizers, electrochemical methods for the production of inorganic metal compounds by electrolysis of aqueous solutions, the production of soda, aqueous solutions of inorganic substances are widely used. For the effective use of aqueous solutions of electrolytes in these areas of technology, accurate information is required on their thermophysical properties, in particular, on thermal conductivity and dynamic viscosity in a wide range of state parameters. In modern technology, a variety of fluids are used as heat carriers. However, it is not always possible to timely obtain experimental data on the physical properties of these substances at high state parameters. This is especially true for thermal conductivity and dynamic viscosity, the experimental determination of which presents significant difficulties. Therefore, it is important to consider the equations that are the most reliable and convenient for calculation with sufficient approximation for practice [14,15].

2 Method

Cooling fluids are used in many industrial fields such as electronics, refrigeration, air conditioning equipment and transportation. The thermal conductivity of these fluids plays a vital role in the development of high-performance heat transfer devices. Since solids have much higher thermal conductivity than conventional fluids, the idea of introducing heat-conducting particles into the fluid was considered. The thermophysical parameters measured include the thermal conductivity, thermal diffusivity, and specific heat capacity.

In this method the geothermal energy has developed on the thermophysical properties of geothermal waters, namely, on the thermal conductivity and viscosity of aqueous salt solutions at temperatures of 293–473 K, pressures Ps = 100 MPa, and concentrations of 0–25 wt.%. For this purpose a generalized formula for obtaining reliable data on the thermal conductivity of water in the pressure ranges Ps = 1000 MPa, temperatures of 293–473 K and the thermal conductivity of aqueous solutions of salts in the pressure ranges Ps = 100 MPa, temperatures of 293–473 K and concentrations of 0%–25% (wt.%), as well as generalized formulas for the dynamic viscosity of water up to pressures of 500 MPa and aqueous solutions of salts in the pressure ranges Ps = 100 MPa, temperatures 333–473 K, and concentration 0%–25%.

Maxwell was the first person who investigated thermal conductiv- ity, using particle suspension system. Maxwell's model ignores the in- teractions between particles and the base fluid and assumes very low concentration of spherical particles. Other researchers have investigated the effects of different parameters such as particle morphology, surface energy, and heat resistance on thermal conductivity. Table 2 shows some of the current theoretical and empirical models used for nanoparticles. As can be seen, changes in thermal conductivity are dependent on volume fraction and temperature of nanofluids. high mineralized waters with purities of 99.9% and 99.5%, respectively, were used in the current study. An

important challenge with nanofluids is that nanoparticles tend to accumulate due to molecular interactions such as van der Waals forces [16–21]. Therefore, as the percentage of filler increases, the accumulation of particles also increases. Also, the viscosity of the system increases and with decreasing the ratio of the effective surface area to the volume, the thermal performance of the fluid also decreases. In general, the accumulation velocity is determined by the collision frequency and the probability of cohesion during collision.

3 Results

3.1 Thermal Conductivity

For aqueous solutions of binary and multicomponent inorganic substances, in [4,5] proposed a formula for determining the coefficient of thermal conductivity of aqueous solutions of salts, acids, and alkalis at a temperature of 293 K without the coefficient 1.163–for a unit of measurement of thermal conductivity in kcal/(m·h·deg), and the author of this paper introduced 1.163 to measure the thermal conductivity coefficient in W/(m·K):

$$\lambda^E(N, T = 293) = \lambda^W(T = 293) + 1.163 \sum_i a_i N_i, \tag{1}$$

where 1.163–the coefficient of conversion of the unit of measurement of thermal conductivity from kcal/(m·h·deg) to W/(m·K). Typical coefficients (a_i) are given in [4,5], and here they are presented in Table 1.

Table 1: The characteristic coefficients (a_i) for each ion, determined by Riedel [17]

Anion	a_i	Cation	a_i
OH^-	+0.0180[3*]	H^+	–0.0078
F^-	+0.0018**	Li^+	–0.0030**
Cl^-	–0.0047	Na^+	0.0000
Br –	–0.0150	K^+	–0.0065
I^-	–0.0236	NH_4^+	–0.0100[4*]
NO_2^-	–0.0040	Mg^{2+}	–0.0080
NO_3^-	–0.0060	Ca^{2+}	–0.0005
ClO_3^-	–0.0122*	Sr^{2+}	–0.0034
ClO_4^-	–0.0150*	Ba^{2+}	–0.0066
BrO_3^-	–0.0122*	Ag^+	–0.0090*
CO_3^{2-}	–0.0065[3*]	Cu^{2+}	–0.0140[4*]
SiO_3^{2-}	–0.0080*	Zn^{2+}	–0.0140[4*]
SO_3^{2-}	–0.0020*	Pb^{2+}	–0.0080[4*]
SO_4^{2-}	+0.0010	Co^{2+}	–0.0100*
$S_2O_3^{2-}$	–0.0070[3*]	Al^{3+}	–0.0280*
CrO_4^{2-}	+0.0010*	Th^{4+}	–0.0375*
$Cr_2O_7^{2-}$	–0.0137*		

Notes: * – the a_i value was determined on the basis of experimental data for only one solution and is not entirely reliable; **–deviations in the area of high concentrations are possible; [3*]–can be applied to concentrations below 1 mol/l; [4*]–the value is unreliable (little experimental data).

Note that $N = 10\ rc/m$ [3], where N is the concentration of the electrolyte, mol/dm^3 of the solution; r–solution density, g/dm^3; c–solution concentration, wt.%; m–the molar mass of the substance, g/mol. Data on the density of solutions of various water-salt systems and molar masses are given in [6], and a_i – coefficients characteristic for each ion are presented in [4], and here in Table 2.

Table 2: Coefficients of thermal conductivity of aqueous solutions of electrolytes at a temperature of 293 K [17]

System	5%	10%	20%	30%	40%	50%
LiOH	615	621				
$NaOH + H_2O$**	614	627	640	645		647
$KOH + H_2O$**	601	604	599	584	564	536
$HCl + H_2O$	579	558	511	463		
$HNO_3 + H_2O$*	583	574	548	521	498	
$H_2SO_4 + H_2O$	590	580	558	534	506	474
$H_2CrO_4 + H_2O$	591	581	562	541	518	488
$H_3PO_4 + H_2O$	587	579	557	533	509	486
$LiCl + H_2O$	588	577	553	538		
$LiBr + H_2O$	586	572	542	507	471	
$LiI + H_2O$*	586	572	541	506	468	427
$LiSO_4 + H_2O$	597	593	587			
$NaCl + H_2O$	594	590	578			
$NaBr + H_2O$*	591	590	558	534	504	
$NaI + H_2O$*	590	579	556	528	494	452
$NaNO_2 + H_2O$	595	592	584	574	561	
$NaNO_3 + H_2O$	595	591	580	569	556	
$Na_2SO_3 + H_2O$	598	597	593			
$Na_2SO_4 + H_2O$	599	600				
$Na_2S_2O_3 + H_2O$	597	593	585	570	544	
$Na_2CO_3 + H_2O$	602	607				
$Na_2SiO_3 + H_2O$	602	607	617			
$Na_3PO_4 + H_2O$	606	613				
$NaClO_3 + H_2O$	592	585	569	550	529	
$NaClO_4 + H_2O$*	591	583	563	547	523	498
$NaBrO_3 + H_2O$	593	588	577			
$Na_2Cr_2O_7 + H_2O$	595	593	583	577	568	558
$KF + H_2O$	594	588	572	545		
$KCl + H_2O$	590	580	559			
$KBr + H_2O$	588	576	550	519	484	
$KI + H_2O$	588	576	550	519	481	436

(Continued)

Table 2 (continued)

System	5%	10%	20%	30%	40%	50%
$KNO_2 + H_2O$*	592	584	566	547	527	508
$KNO_3 + H_2O$	592	584	566			
$K_2SO_4 + H_2O$	594	590				
$K_2CO_3 + H_2O$*	595	592	583	564	540	509
$K_2(COO)_2 + H_2O$*	593	587	573			
$K_4Fe(CN)_6 + H_2O$*	592	584	567			
$MgCl_2 + H_2O$	586	573	547	516		
$MgBr_2 + H_2O$*	586	573	542	505	459	407
$Mg(NO_3)_2 + H_2O$*	591	583	564	542		
$MgSO_4 + H_2O$	595	592	583			
$CaCl_2 + H_2O$	593	587	576	561	545	
$CaBr_2 + H_2O$*	590	579	556	529	495	454
$Ca(NO_3)_2 + H_2O$*	594	590	578	565	550	533
$SrCl_2 + H_2O$*	594	588	576	562		
$SrBr_2 + H_2O$*	591	581	561	536	506	467
$Sr(NO_3)_2 + H_2O$	594	590	579	566	550	
$BaCl_2 + H_2O$	594	590	578			
$BaBr_2 + H_2O$	591	583	564	542	515	
$BaI_2 + H_2O$*	590	580	560	534	502	463
$AgNO_3 + H_2O$	593	587	575	558	540	514
$CuSO_4 + H_2O^{3*}$	593	587				
$ZnSO_4 + H_2O$**	593	587	575	559		
$ZnCl_2 + H_2O$*	588	577	551	521	486	
$Pb(NO_3)_2 + H_2O^{3*}$	594	590	579	566		
$Co(NO_3)_2 + H_2O$	592	584	565	544	520	
$Al_2(SO_4)_3 + H_2O$	590	580	555			
$Th(NO_3)_4 + H_2O$	591	583	563			
$NH_4Cl + H_2O^{4*}$	583	566	531			
$NH_3 + H_2O^{5*}$	566	535	484	445		

Note: Table 2 shows the data obtained by Riedel on the thermal conductivity of electrolytes according to formula (1).

In formula (1), there is the letter N–the concentration of the electrolyte, mol/dm^3 of the solution, which is needed in calculations when converting the concentration of the solution near the saturation line from mol/dm^3 to % (wt). For this purpose, the author used the formula $N = r10c/m$ and experimental and reference data [18].

In [19], it considered a formula for calculating the thermal conductivity of aqueous solutions of salts of acids and alkalis at temperatures of 293–373 K. The formula for the equality of the same ratios of the thermal conductivity of water and aqueous solutions at T = 273–373 K is the following:

$$\frac{\lambda^W(T)}{\lambda^W(T=293)} = \frac{\lambda^E(N,T)}{\lambda^E(N,T=293)}. \tag{2}$$

The author's studies have shown that formula (2) can be represented as (3) and (4) when using the values of thermal conductivity of water and aqueous solutions of electrolytes near the saturation line at temperatures of 293–473 K. If instead $\lambda^E(N, T = 293)$, one substitutes into formula (2) the value of formula (1), then formulas (3) and (4) are obtained, for calculating the thermal conductivity of aqueous solutions of salts near the saturation line in the temperature ranges of 293–473 K and pressures of 0.1–2 MPa.

Equation formulas for the ratio of thermal conductivity of water and aqueous solutions of electrolytes at temperatures of 273–473 K [5] are the following:

$$\frac{\lambda^W(P_S,T)}{\lambda^W(T=293)} = \frac{\lambda^E(P_S,N,T)}{\lambda^E(N,T=293)}, \tag{3}$$

$$\lambda^E(P_S,N,T) = \frac{\lambda^W(P_S,T)}{\lambda^W(T=293)} \times \left[\lambda^W(T=293) + 1.163\sum_i a_i N_i\right]$$

$$= \lambda^W(P_S,T)\left[1 + 1.938\sum_i a_i N_i\right], \tag{4}$$

The deviation of the calculated values of the thermal conductivity of aqueous salt solutions near the saturation line according to formula (4) from the experimental data [4,5,9] was less than 1.3%, and from the data according to formula (1) at a temperature of 293 K, less than 1% (because formula (1) is only for one temperature–293 K).

The effect of salt on the thermal conductivity of the solution is manifested in the same way at all temperatures, when taking the interval of 293–473 K at pressures of 0.1–2 MPa.

In calculations by formula (4), critically estimated experimental values of the thermal conductivity of water in a state of saturation [22] were used, and the characteristic coefficients for each ion a_i were those from [4] (given in Table 1) and new ones, which were obtained by the author using formula (4).

Note that a_i for most aqueous solutions of salts, acids, and alkalis (anions and cations) consist of negative numbers.

Based on the analysis of the obtained formulas and data from various works on the thermal conductivity of aqueous solutions of inorganic substances [23], a generalized formula (5) was obtained for calculating the thermal conductivity (W/(m·K)) of aqueous solutions of salts [24] in the temperature range of 293–473 K, pressures of 0.1–100 MPa, and concentrations of 0–25 wt.%.

Table 3: $A_i \times 10^5$ are the coefficients characteristic of each water-salt system

System	$A_i \cdot 10^5$	μ [6]	System	$A_i \cdot 10^5$	μ [6]
$AgF + H_2O$	119	126.866	$KI + H_2O$	380	166.003
$KF + H_2O$	185	58.096	$LiI + H_2O$	417	133.846
$KCl + H_2O$	315	74.551	$NaI + H_2O$	310	149.894
$LiCl + H_2O$	380	42.394	$NH_4I + H_2O$	487	144.943
$NaCl + H_2O$	168	58.443	$RbI + H_2O$	317	212.372
$RbCl + H_2O$	229	120.921	$BaI_2 + H_2O$	289	391.139
$BaCl_2 + H_2O$	160	208.236	$CaI_2 + H_2O$	340	293.889
$CaCl_2 + H_2O$	187	110.986	$CoI_2 + H_2O$	384	312.813
$CdCl_2 + H_2O$	170	183.316	$MgI_2 + H_2O$	417	278.113
$CoCl_2 + H_2O$	314	129.839	$NiI_2 + H_2O$	392	312.496
$CuCl_2 + H_2O$	350	134.452	$SrI_2 + H_2O$	310	341.425
$FeCl_2 + H_2O$	280	126.753	$ZnI_2 + H_2O$	403	319.189
$FeCl_3 + H_2O$	286	162.206	$HNO_3 + H_2O$	350	63.012
$MgCl_2 + H_2O$	384	95.211	$AgNO_3 + H_2O$	185	169.872
$MnCl_2 + H_2O$	265	125.844	$KNO_3 + H_2O$	260	101.102
$NiCl_2 + H_2O$	330	129.606	$LiNO_3 + H_2O$	274	68.945
$SrCl_2 + H_2O$	170	158.526	$NaNO_3 + H_2O$	148	84.994
$ZnCl_2 + H_2O$	360	136.286	$RbNO_3 + H_2O$	206	147.480
$NaClO_3 + H_2O$	240	106.440	$Ca(NO_3)_2 + H_2O$	160	164.087
$NaClO_4 + H_2O$	250	122.438	$Cd(NO_3)_2 + H_2O$	155	236.417
$K_2CrO_4 + H_2O$	130	194.190	$Co(NO_3)_2 + H_2O$	252	182.941
$Na_2CrO_4 + H_2O$	–13	161.972	$Cu(NO_3)_2 + H_2O$	280	187.553
$Na_2S_2O_3 + H_2O$	93	158.110	$Mg(NO_3)_2 + H_2O$	283	148.312
$KBr + H_2O$	362	119.002	$Ni(NO_3)_2 + H_2O$	255	182.717
$LiBr + H_2O$	410	86.845	$Pb(NO_3)_2 + H_2O$	127	331.224
$NaBr + H_2O$	280	102.894	$Sr(NO_3)_2 + H_2O$	153	211.627
$NH_4Br + H_2O$	514	97.942	$Zn(NO_3)_2 + H_2O$	288	189.387
$RbBr + H_2O$	286	165.372	$CoSO_4 + H_2O$	118	154.989
$BaBr_2 + H_2O$	244	297.138	$CuSO_4 + H_2O$	168	159.602
$CaBr_2 + H_2O$	297	199.888	$MgSO_4 + H_2O$	122	120.361
$CdBr_2 + H_2O$	258	272.218	$NiSO_4 + H_2O$	121	154.756
$CoBr_2 + H_2O$	364	218.741	$ZnSO_4 + H_2O$	169	161.436
$FeBr_2 + H_2O$	350	215.655	$Li_2SO_4 + H_2O$	96	109.938
$MgBr_2 + H_2O$	410	184.113	$(NH_4)_2SO_4 + H_2O$	302	132.133
$NiBr_2 + H_2O$	362	218.496	$NaBrO_3 + H_2O$	170	150.891
$SrBr_2 + H_2O$	266	247.428	$H_2SO_4 + H_2O$	290	98.077
$ZnBr_2 + H_2O$	392	225.210	$H_2CrO_4 + H_2O$	260	118.009

Note: $A_i \times 10^5$–coefficients typical for each binary system of aqueous solutions of inorganic substances are presented here and in [4,5,9,25–29].

$$\lambda^E(P,T,c) = \lambda^W(P,T)\left[\left(1 - \sum_i A_i\left(c_i + 2\times 10^{-4}c^3\right)\right) - 2\times 10^{-8}PT\sum_i c_i\right], \quad (5)$$

A_i – coefficients characteristic of each binary system of aqueous solutions of inorganic substances, determined from experimental data on the thermal conductivity of the solution are presented in Table 3 and in [25–28].

Formula (6) for calculating the thermal conductivity of water and aqueous salt solutions at T = 273–473 K is presented in [30]:

$$\lambda^E(P,T,c) = \lambda^E(P_s,T,c)\left[\left(1.7\frac{\rho^W(P,T)}{\rho^W(P_S,T)} - 0.7\right) - 2.5\times 10^{-8}PT\sum_i c_i\right], \quad (6)$$

and for pure water (c = 0), formula (6) takes the form of formula (7):

$$\lambda^W(P,T) = \lambda^W(P_s,T)\left(1.7\frac{\rho^W(P,T)}{\rho^W(P_S,T)} - 0.7\right), \quad (7)$$

where P_s is the pressure near the saturation line, which during the experiment can be $0.1 \le P_s \le 2.0$ MPa at experiment temperatures $273 \le T \le 473$ K.

3.2 Dynamic Viscosity

Based on the analysis of the density data of pure water and experimental data on the dynamic viscosity of aqueous solutions of salts of various authors, a new generalized formula is presented that can be used to obtain the values of the viscosity of aqueous solutions of salts in the temperature range of 333–473 K, pressures of 0.1–100 MPa, and concentrations of 0–25 wt.%.

The viscosity of saline waters has not been studied sufficiently at high pressures. The material on the dynamic viscosity of water-salt systems at pressures above 40 MPa is limited. There is no reference material on the dynamic viscosity of water-salt systems at pressures of 40–100 MPa.

Based on the analysis of density data [31], viscosity [32] of pure water, and experimental data on the dynamic viscosity of aqueous solutions of salts of various authors [33], a new generalized formula (8) is presented, which can be used to obtain the values of viscosity (μPa·s) of aqueous solutions of salts in the temperature range of 333–473 K, pressures of 0.1–100 MPa, and concentrations of 0–25 wt.%–in the presence of viscosity data near the saturation line. The formula is as follows:

$$\eta^E(P,T,c) = \eta^E(P_s,T,c)\left[\left(1.7\frac{\rho^W(P,T)}{\rho^W(P_S,T)} - 0.7\right) - 2.5\times 10^{-8}PTc\right] + \\ +1.6\times 10^{-4}\frac{PT}{P_1T_1}, \quad (8)$$

and for pure water (c = 0) formula (8) takes the form:

$$\eta^W(P,T) = \eta^W(P_s,T)\left(1.7\frac{\rho^W(P,T)}{\rho^W(P_S,T)} - 0.7\right) + 1.6\times 10^{-4}\frac{PT}{P_1T_1}, \quad (9)$$

where $\eta^W(P_s,T,c)$ is the coefficient of dynamic viscosity of the solution (μPa·s) at pressure P, MPa, temperature T, K and concentration c, wt.%; $\eta^E(P_s,T,c)$–the viscosity of the solution near the saturation line at T and c; $\rho^W(P,T)$, $\eta^W(P,T)$–density and viscosity of pure water at P and T; $\rho^W(P_S,T)$, $\eta^W(P_s,T)$

are the density and viscosity of water near the saturation line at P_s and T; P_s is the pressure at the saturation line; $c = \sum_{i=1} c_i$, wt.%, where c_i is the concentration of the i-th system; P_1 =1 MPa; T_1 = 1 K.

Table 4: Thermal conductivity values according to formula (5) of the multicomponent system H_2O + NaCl + $MgCl_2$ + $CaCl_2$

T, K	P, MPa; $\lambda \cdot 10^3$, W/(m·K)					
	Ps	20	40	60	80	100
	2% NaCl + 2% $MgCl_2$ + 1% $CaCl_2$ + H_2O					
293.15	593	602	610	618	626	634
313.15	623	632	640	649	657	664
333.15	644	653	661	670	679	687
353.15	660	669	679	688	696	705
373.15	670	680	691	700	709	718
393.15	679	690	701	712	721	731
423.15	676	689	701	712	723	733
473.15	654	670	687	700	714	726
	4% NaCl + 4% $MgCl_2$ + 2% $CaCl_2$ + H_2O					
293.15	585	593	601	608	615	622
313.15	615	622	631	638	646	652
333.15	635	643	651	658	666	672
353.15	652	660	669	676	685	692
373.15	662	671	681	688	697	704
393.15	667	677	687	696	704	712
423.15	667	679	690	700	710	719
473.15	646	661	676	690	702	713
	5% NaCl + 5% $MgCl_2$ + 5% $CaCl_2$ + H_2O					
293.15	579	587	594	601	607	614
313.15	608	615	623	630	637	643
333.15	629	636	644	652	658	664
353.15	645	652	661	668	675	682
373.15	654	663	671	679	686	693
393.15	660	669	678	686	694	702
423.15	660	671	681	690	700	708
473.15	639	653	668	680	691	702

Note: Values in Table 4 agree with [30] within 1.3%.

Table 5: The values of the dynamic viscosity of water calculated by formula (9), μPa·s at high temperatures and pressures

P, MPa	*T*, K						
	333.15	348.15	373.15	398.15	423.15	448.15	473.15
P_s	465.0	377.9	281.8	221.0	182.5	156.1	134.3
20	473.1	384.7	287.5	226.6	187.6	161.0	139.4
40	480.1	391.4	293.2	231.0	192.3	165.9	144.3
60	487.7	397.4	298.4	235.9	196.8	170.4	148.9
80	495.3	403.8	303.5	240.5	201.2	174.9	153.3
100	501.0	409.6	308.6	245.1	205.5	178.9	157.5
120		415.6	313.2	249.4	209.6	183.1	161.5
140		421.2	318.1	253.5	213.5	186.9	165.4
160		426.5	322.7	257.5	217.4	190.7	169.2
180		431.7	326.9	261.7	221.3	194.4	172.7
200		437.0	331.2	265.3	224.8	197.9	176.4
220		442.0	335.5	269.3	228.4	201.6	180.0
240		447.2	339.8	273.0	231.9	205.0	183.4
260		452.1	343.8	276.7	235.5	208.3	186.6
280		456.6	347.8	280.1	238.9	211.6	189.9
300		461.5	351.8	283.6	242.2	214.8	193.0
320		466.4	355.8	287.4	245.4	217.9	196.1
340		470.9	359.3	290.7	248.4	221.1	199.1
360		475.3	363.0	293.8	251.8	224.4	202.3
380		479.8	366.8	297.1	254.9	227.2	205.1
400		484.1	370.5	300.4	258.0	230.5	208.2

Note: The calculated values of the dynamic viscosity of pure water according to formula (9) are consistent industrial standard [10] and the recommended reference data [11] in the temperature range of 348–473 K and pressures of 0.1–100 MPa within 1%, and in the temperature range of 348–473 K and pressures of 100–300 MPa within 1.5%.

Table 6: The values of the dynamic viscosity of the $H_2O + Na_2SO_4$ system calculated by formula (8) at high temperatures, pressures, and concentrations. η, μPa·s

T, K	*P*, MPa					
	P_s	20	40	60	80	100
	c = 1.5 wt.%					
348.2	395.0	402.8	410.2	416.9	423.8	430.8
373.8	292.0	297.9	303.7	308.7	314.0	319.3
398.0	229.5	234.9	239.8	244.5	249.3	254.0
422.6	190.4	195.6	200.6	204.9	209.5	213.7

(Continued)

Table 6 (continued)

T, K	P, MPa					
	P_s	20	40	60	80	100
			c = 1.5 wt.%			
447.6	160.9	165.7	170.5	175.1	179.6	183.5
470.7	140.9	145.6	149.7	155.8	160.4	164.6
	c = 5 wt.%					
347.2	443.4	450.9	458.0	464.4	471.7	477.8
372.0	329.0	335.1	341.3	346.7	352.2	357.7
395.6	259.9	265.6	270.7	275.9	280.9	285.8
424.7	205.4	210.7	215.7	220.4	225.6	229.4
446.2	176.9	182.1	187.2	192.0	196.7	200.2
470.2	153.9	159.3	164.6	170.9	174.0	178.4
	c = 10 wt.%					
348.4	523.2	531.1	539.1	546.4	553.8	560.2
372.4	391.6	398.3	404.5	410.9	417.1	423.0
398.7	302.4	308.5	314.0	319.5	324.7	330.0
421.4	250.7	256.6	262.2	267.3	272.4	277.0
447.2	209.5	215.2	220.8	225.7	230.9	235.3
471.3	181.9	187.9	193.4	198.8	203.8	208.4
	c = 15 wt.%					
348.7	629.2	637.9	647.1	654.5	663.2	670.0
372.8	466.7	474.0	481.2	487.0	494.4	500.7
395.4	369.7	376.5	382.6	388.6	394.4	400.1
421.3	296.5	302.9	309.0	314.2	319.7	324.9
447.8	246.1	252.3	257.9	263.7	269.3	273.7
473.9	210.1	216.3	222.6	228.0	233.4	238.3
	c = 20 wt.%					
347.9	789.2	799.8	809.6	818.5	827.5	835.8
374.5	565.3	573.3	581.8	588.7	595.5	602.4
397.2	446.4	453.9	460.5	467.2	473.4	479.6
472.3	256.9	263.9	270.9	277.1	282.8	288.1
	c = 26 wt.%					
348.6	1010.0	1022.0	1034.0	1044.0	1055.0	1064.0
375.2	725.8	735.4	745.3	753.4	761.1	769.5
399.4	564.4	573.6	581.6	588.0	595.5	602.4
423.8	457.5	465.8	474.0	481.0	487.7	494.1
447.6	385.7	393.8	401.7	408.1	415.7	421.1
473.9	325.9	334.3	342.4	349.3	355.8	362.2

Note: The calculated values of the dynamic viscosity according to formula (1) agree with the experimental data [18] within 1.4%.

Table 7: The values of the dynamic viscosity of the H_2O + NaCl system calculated by formula (8) at high temperatures, pressures and concentrations. η, μPa·s

T, K	P, MPa					
	P_s	20	40	60	80	100
				c = 5 wt.%		
323	680.0	617.5	626.4	635.3	643.6	651.9
373	320.4	326.4	332.4	337.8	343.1	348.5
423	209.8	215.2	220.3	225.0	229.7	234.2
473	155.9	161.4	166.7	171.5	175.6	180.6
	c = 10 wt.%					
323	678.8	688.9	698.4	706.9	716.1	724.5
373	362.1	368.3	374.4	380.0	385.7	391.2
423	237.9	243.6	248.9	253.9	258.7	263.5
473	175.8	181.6	187.0	192.2	197.2	201.7
	c = 15 wt.%					
323	757.0	767.8	777.2	786.5	795.1	804.4
373	412.3	418.9	425.4	431.6	437.3	443.0
423	270.2	276.2	281.8	286.7	291.2	296.7
473	200.2	206.2	212.2	217.5	222.7	227.4
	c = 20 wt.%					
323	856.2	867.5	877.9	886.6	896.2	905.7
373	469.5	476.3	483.6	489.5	495.4	501.3
423	303.8	310.3	315.9	321.0	326.2	331.6
473	224.9	231.2	237.6	243.1	248.3	253.2

Note: The calculated values of the dynamic viscosity according to formula (8) agree with the experimental data [18] within 1%.

Table 8: The values of the dynamic viscosity of the H_2O + $CaCl_2$ system calculated by formula (1) at high temperatures, pressures and concentrations. η, μPa·s

T, K	P, MPa					
	P_s	10	30	60	80	100
				c = 9.72 wt.% or 0.97 mol/kg		
348.74	521	525	533	544	551	558
399.44	313	316	322	331	336	341
424.74	259	262	268	276	281	286
446.48	225	228	234	242	247	252
470.94	196	199	205	214	219	224
	c = 18.17 wt.% or 2.00 mol/kg					
349.02	722	727	736	750	758	766
372.09	559	564	571	582	589	596
397.74	441	445	453	462	468	474

(Continued)

Table 8 (continued)

T, K	*P*, MPa					
	P_s	10	30	60	80	100
			c = 9.72 wt.% or 0.97 mol/kg			
427.76	361	365	373	382	388	393
448.94	307	312	319	327	333	339
474.06	268	272	279	288	294	300

Note: The calculated values of the dynamic viscosity according to formula (8) agree with the experimental data [13] within 1.6%.

According to formula (8), the values of the dynamic viscosity of various water-salt systems were obtained in the temperature range of 333–473 K, pressures of 0.1–100 MPa, and concentrations of 0–25 wt.%. The deviation of the calculated values of the viscosity of water-salt systems according to formula (1) from the experimental data of various authors [30] was less than 1.5%. Here, in Tables 5–9, the values of dynamic viscosity for five water-salt systems are presented, although many systems have been studied, and Figs. 1 and 2 show isobars of water and aqueous solutions of sodium chloride.

Note that there are experimental studies of water-salt systems by various authors at pressures up to 40 MPa and a small part up to 60 MPa.

Table 9: The values of the dynamic viscosity of the H_2O + LiCl system calculated by formula (1) at high temperatures, pressures and concentrations, η, μPa·s

T, K	*P*, MPa					
	P_s	10	30	60	80	100
			c = 5 wt.%			
348.15	454	461	469	476	483	489
420.25	264	270	275	280	285	290
470.42	166	172	177	182	187	192
	c = 10 wt.%					
399.72	326	333	339	344	350	355
452.54	226	232	238	244	249	254
	c = 20 wt.%					
348.15	842	854	864	873	883	891
397.20	514	522	530	537	544	551
447.18	363	371	379	386	392	398
471.50	317	326	335	342	348	354

Note: The calculated values of the dynamic viscosity according to formula (8) agree with the experimental data [6] within 1.6%.

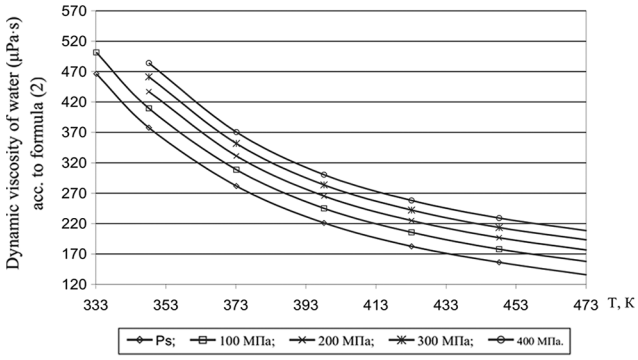

Figure 1: Viscosity of water at high state parameters

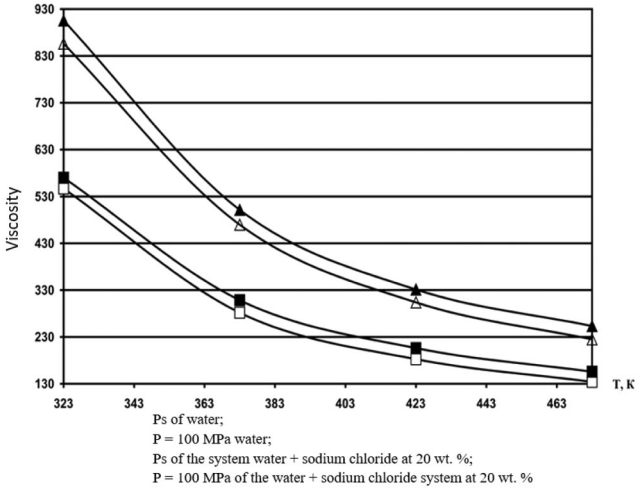

Figure 2: Isobar viscosity of water and aqueous solutions of sodium chloride, calculated by formula (1) at 20 wt.%

4 Conclusion

In the present paper Based on the analysis of experimental data, generalized formulas are presented, which in turn will allow many scientists to use them to obtain reliable and accurate material on the thermal conductivity and dynamic viscosity of aqueous solutions of salts. Nanofluids are a new generation of fluids with great potential in industrial cartridges. In nanofluids, due to the small size of the particles, a significant amount of corrosion, impurities and pressure drop problems are reduced and the stability of fluids against sedimentation is significantly improved. To increase the stability of nanofluid suspension in order to increase the thermal conductivity, surfactants and physical or chemical bonding of polymer chains on the surface of nanostructures can be used. Other factors affecting the thermal conductivity of the nanofluid include the amount of nano filler, the viscosity of the nanofluid and the temperature of the system used. The presence of nanofillers in the nanofluid changes the thermal conductivity by changing the temperature, whereas without the filler the thermal conductivity is not temperature dependent. Results demonstrated that thermal conductivity of Water hybrid nanofluid increases with increase in volume fraction of nanoparticles.Also, based on the experimental results of the previous researches a novel a novel correlation with a margin of deviation of 1.6% was proposedfor predicting thermal conductivity.

Funding Statement: The authors received no specific funding for this study.

Conflicts of Interest: The authors declare that they have no conflicts of interest to report regarding the present study.

References

1. Zainal, A. G., Yulianto, H., Yanfika, H. (2021). Financial benefits of the environmentally friendly aquaponic media system. *IOP Conference Series: Earth and Environmental Science,* vol. 739, 012024. IOP Publishing.
2. Gashi, F., Dreshaj, E., Troni, N., Maxhuni, A., Laha, F. (2020). Determination of heavy metal contents in water of Llapi River (Kosovo). A case study of correlations coefficients. *European Chemical Bulletin, 9(2),* 43–47. DOI 10.17628/ecb.2020.9.43-47.
3. Chen, H., Bokov, D., Chupradit, S., Hekmatifar, M., Mahmoud, M. Z. et al. (2021). Combustion process of nanofluids consisting of oxygen molecules and aluminum nanoparticles in a copper nanochannel using molecular dynamics simulation. *Case Studies in Thermal Engineering, 28(3),* 101628. DOI 10.1016/j.csite.2021.101628.
4. Prischepa, O. M., Nefedov, Y. V., Ibatullin, A. K. (2020). Raw material source of hydrocarbons of the arctic zone of russia. *Periodico Tche Quimica, 17(36),* 506–526. DOI 10.52571/PTQ.v17.n36.2020.521_Periodico36_pgs_506_526.pdf.
5. Al-Hassani, K. A., Alam, M. S., Rahman, M. M. (2021). Numerical simulations of hydromagnetic mixed convection flow of nanofluids inside a triangular cavity on the basis of a two-component nonhomogeneous mathematical model. *Fluid Dynamics & Materials Processing, 17(1),* 1–20. DOI 10.32604/fdmp.2021.013497.
6. Alkhasov, A. B., Magomedov, U. B., Magomedov, M. M. S. (2011). Thermal conductivity of aqueous solutions of salts at high state parameters. *Natural and Technical Sciences, 1(51),* 23–26.
7. Yang, S., Jasim, S. A., Bokov, D., Chupradit, S., Nakhjiri, A. T. et al. (2021). Membrane distillation technology for molecular separation: A review on the fouling, wetting and transport phenomena. *Journal of Molecular Liquids, 565(2),* 118115. DOI 10.1016/j.molliq.2021.118115.
8. Anggono, A. D., Elveny, M., Abdelbasset, W. K., Petrov, A. M., Ershov, K. A. et al. (2021). Creep deformation of $Zr_{55}Co_{25}Al_{15}Ni_5$ bulk metallic glass near glass transition temperature: A nanoindentation study. *Transactions of the Indian Institute of Metals,* 1–8.
9. Nourdanesh, N., Ranjbar, F. (2022). Investigation on heat transfer performance of a novel active method heat sink to maximize the efficiency of thermal energy storage systems. *Journal of Energy Storage, 45(12),* 103779. DOI 10.1016/j.est.2021.103779.
10. Nourdanesh, N., Ranjbar, F. (2021). Introduction of a novel electric field-based plate heat sink for heat transfer enhancement of thermal systems. *International Journal of Numerical Methods for Heat & Fluid Flow,* 61. DOI 10.1108/HFF-08-2021-0531.
11. Magomedov, U. B. (2005). Thermal conductivity of aqueous solutions of inorganic substances at high temperatures, pressures and concentrations. *Materials of the International Conference Renewable Energy: Problems and Prospects,* vol. 2, pp. 115–123. Makhachkala: Delovoi mir.
12. Mozaffari, M., D'Orazio, A., Karimipour, A., Abdollahi, A., Safaei, M. R. (2019). Lattice Boltzmann method to simulate convection heat transfer in a microchannel under heat flux: Gravity and inclination angle on slip-velocity. *International Journal of Numerical Methods for Heat & Fluid Flow, 30(6),* 3371–3398. DOI 10.1108/HFF-12-2018-0821.
13. Abdulagatov, I. M., Azizov, N. D. (2006). Viscosity of aqueous calcium chloride solutions at high temperatures and high pressures. *Fluid Phase Equilibria, 240(2),* 204–219. DOI 10.1016/j.fluid.2005.12.036.
14. Sun, K., Hu, X., Li, D., Zhang, G., Zhao, K. et al. (2021). Analysis of bubble behavior in a horizontal rectangular channel under subcooled flow boiling conditions. *Fluid Dynamics & Materials Processing, 17(1),* 81–95. DOI 10.32604/fdmp.2021.013895.
15. Han, Y. (2020). Investigation of reynolds number effects on high-speed trains using low temperature wind tunnel test facility. *Fluid Dynamics & Materials Processing, 16(1),* 1–19. DOI 10.32604/fdmp.2020.06525.

16. Abdulagatov, I. M., Azizov, N. D. (2005). Viscosity of aqueous LiI solutions at 293-523 K and 0.1–40 MPa. *Thermochimica Acta, 439(1–2),* 8–20. DOI 10.1016/j.tca.2005.08.036.
17. Abdulagatov, I. M., Zeinalova, A. B., Azizov, N. D. (2004). Viscosity of the aqueous Ca $(NO_3)_2$ solutions at temperatures 298 to 573 K and at pressures up to 40 MPa. *Journal of Chemical Engineering Data, 49(5),* 1444–1450. DOI 10.1021/je049853n.
18. Abdulagatov, I. M., Zeinalova, A. B., Azizov, N. D. (2006). Experimental viscosity B-coefficients of aqueous LiCl solutions. *Journal of Molecular Liquids, 126(1–3),* 75–88. DOI 10.1016/j.molliq.2005.10.006.
19. Akmedova-Azizova, L. A. (2006). Thermal conductivity and viscosity of aqueous $Mg(NO_3)_2$, $Ca(NO_3)_2$ and Ba $(NO_3)_2$ solutions at high temperatures and high pressures. *Journal of Chemical Engineering Data, 54,* 510–517.
20. Tian, Z., Bagherzadeh, S. A., Ghani, K., Karimipour, A., Abdollahi, A. et al. (2019). Nonlinear function estimation fuzzy system (NFEFS) as a novel statistical approach to estimate nanofluids' thermal conductivity according to empirical data. *International Journal of Numerical Methods for Heat & Fluid Flow, 30(6),* 3267–3281. DOI 10.1108/HFF-12-2018-0768.
21. Hoseini, M., Haghtalab, A., Navid Family, M. (2020). Elongational behavior of silica nanoparticle-filled low-density polyethylene/polylactic acid blends and their morphology. *Rheologica Acta, 59(9),* 621–630. DOI 10.1007/s00397-020-01225-5.
22. Abdulagatov, I. M., Zeinalova, A. B., Azizov, N. D. (2005). Viscosity of aqueous Na_2SO_4 solutions at temperatures from (298 to 573) K and at pressures up to 40 MPa. *Fluid Phase Equilibria, 227(1),* 57–70. DOI 10.1016/j.fluid.2004.10.028.
23. Zeynalova, A. B., Iskenderov, A. I., Tairov, A. D., Akhundov, T. S. (1991). Dynamic viscosity of calcium nitrate. *Oil and Gas Studies, 1,* 53–54.
24. Nikfarjam, A., Raji, H., Hashemi, M. M. (2019). Label-free impedance-based detection of encapsulated single cells in droplets in low cost and transparent microfluidic chip. *Journal of Bioengineering Research, 1(4),* 29–37.
25. Ahmadizadeh, P., Mashadi, B., Lodaya, D. (2017). Energy management of a dual-mode power-split powertrain based on the Pontryagin's minimum principle. *IET Intelligent Transport Systems, 11(9),* 561–571. DOI 10.1049/iet-its.2016.0281.
26. Sokolov, B., Potryasaev, S., Serova, E., Ipatov, Y., Andrianov, Y. (2019). Informative and formal description of structure dynamics control task of cyber-physical systems. *Journal of Applied Engineering Science, 17(1),* 61–64. DOI 10.5937/jaes16-18716.
27. Bakhtiari, R., Kamkari, B., Afrand, M., Abdollahi, A. (2021). Preparation of stable TiO_2-Graphene/Water hybrid nanofluids and development of a new correlation for thermal conductivity. *Powder Technology, 385,* 466–477. DOI 10.1016/j.powtec.2021.03.010.
28. Deryagin, A. V., Krasnova, L. A., Sahabiev, I. A., Samedov, M. N., Shurygin, V. Y. (2019). Scientific and educational experiment in the engineering training of students in the bachelor's degree program in energy production. *International Journal of Innovative Technology and Exploring Engineering, 8(8),* 572–577.
29. Kuzmin, P. A., Bukharina, I. L., Kuzmina, A. M. (2016). The activity of copper-containing enzymes in the birch leaves in the conditions of the built environment. *International Journal of Pharmacy and Technology, 8(4),* 24608–24614.
30. Fedorov, S. N., Smolnikov, A. D., Palyanitsin, P. S. (2020). Metrology and standardization in pressureless flows. *Journal of Physics: Conference Series, 1515(5),* 052069. DOI 10.1088/1742-6596/1515/5/052069.
31. Movchan, I. B., Yakovleva, A. A., Daniliev, S. M. (2019). Parametric decoding and approximated estimations in engineering geophysics with the localization of seismic risk zones on the example of northern part of kola peninsula. *15th Conference and Exhibition Engineering and Mining Geophysics,* pp. 188–198. Gelendzhik.
32. He, W., Bagherzadeh, S. A., Tahmasebi, M., Abdollahi, A., Bahrami, M. et al. (2019). A new method of black-box fuzzy system identification optimized by genetic algorithm and its application to predict mixture thermal properties. *International Journal of Numerical Methods for Heat & Fluid Flow, 30(5),* 2485–2499. DOI 10.1108/HFF-12-2018-0758.
33. Gerdroodbary, M. B., Ganji, D. D., Moradi, R., Abdollahi, A. (2018). Application of knudsen thermal force for detection of CO_2 in low-pressure micro gas sensor. *Fluid Dynamics, 53(6),* 812–823. DOI 10.1134/S0015462818060149.